



Gianluca Rizzi · Geralf Hütter · Angela Madeo ·  
Patrizio Neff

# Analytical solutions of the simple shear problem for micromorphic models and other generalized continua

Received: 6 June 2020 / Accepted: 2 January 2021 / Published online: 28 January 2021  
© The Author(s), under exclusive licence to Springer-Verlag GmbH, DE part of Springer Nature 2021

**Abstract** To draw conclusions as regards the stability and modelling limits of the investigated continuum, we consider a family of infinitesimal isotropic generalized continuum models (Mindlin–Eringen micromorphic, relaxed micromorphic continuum, Cosserat, micropolar, microstretch, microstrain, microvoid, indeterminate couple stress, second gradient elasticity, etc.) and solve analytically the simple shear problem of an infinite stripe. A qualitative measure characterizing the different generalized continuum moduli is given by the shear stiffness  $\mu^*$ . This stiffness is in general length-scale dependent. Interesting limit cases are highlighted, which allow to interpret some of the appearing material parameter of the investigated continua.

**Keywords** Generalized continua · Simple shear · Shear stiffness · Characteristic length · Size-effect · Micromorphic continuum · Cosserat continuum · Gradient elasticity

## 1 Introduction

Today there exists a huge variety of small strain, linear generalized continuum models that allow to extend the modelling capabilities to include size dependent response. We mention Mindlin–Eringen micromorphic [7, 8, 10, 22], relaxed micromorphic continuum [4, 26, 27], Cosserat [3, 17, 25, 28–30], micropolar, microstretch [22, 27], microstrain [11], microvoid [27], indeterminate couple stress [12, 20, 23, 30, 31], second gradient elasticity [22, 29], etc.

The basic problem of all these theories, even for the infinitesimal strain isotropic case under consideration here, is the huge number of newly appearing constitutive coefficient which need to be determined and physically interpreted. Homogeneous tests fail to reveal the inherent size effects, and are therefore not sufficient to determine and interpret those constitutive coefficients that are connected to these size effects. To gain further insight, it is therefore mandatory to investigate boundary value problems which produce some inhomogeneous response (as it can be seen in real or virtual experiments [6, 32–34, 37, 40]). There exist a couple of inhomogeneous analytical solutions to simple shear [1, 2, 5, 9, 14, 16, 18, 19, 21, 34, 39, 41], pure bending and torsion for some of the simpler models mentioned above.

---

G. Rizzi (✉) · A. Madeo  
GEOMAS, INSA-Lyon, Université de Lyon, 20 avenue Albert Einstein, 69621 Villeurbanne cedex, France  
E-mail: gianluca.rizzi@insa-lyon.fr

G. Hütter  
TU Bergakademie Freiberg, Institute of Mechanics and Fluid Dynamics, Lampadiusstr. 4, 09596 Freiberg, Germany

P. Neff  
Head of Chair for Nonlinear Analysis and Modelling, Fakultät für Mathematik, Universität Duisburg-Essen, Thea-Leymann-Straße 9, 45127 Essen, Germany

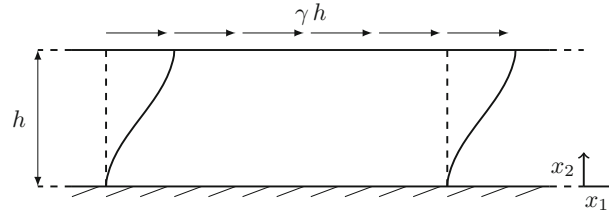


**Fig. 1** Sketch of an infinite stripe subjected to simple shear boundary conditions

Cosserat theory has widely been used to model such size effects since respective analytical solutions are available (and Cosserat has less parameters of course) whereas few analytical solutions are available for more general classes of micromorphic theories (except those which are already cited) and that such solutions are necessary to promote micromorphic theories.

In this paper, we focus on the analytical solution for the simple shear of an infinite stripe, which we provide for a family of generalized continua. The method to obtain these solutions of linear problems is fairly standard, but still needs a concentrated effort. The deep interest occurs in comparing the resulting size-dependent shear stiffness

$$\mu^* = \frac{\tilde{\sigma}_{12}}{\gamma}$$

where  $\tilde{\sigma}$  is force-stress tensor and  $\gamma$  is the shear deformation for the classical shear problem. The factor  $\mu^*$  will, in general, depend on a length-scale parameter ( $L_c \geq 0$ ), the height  $h$  of the stripe (Fig. 1), and on the other parameters of the generalized continua. It is clear that for material samples with infinite relative width (corresponding to  $L_c \rightarrow 0$ , viz  $h \rightarrow \infty$ ), we need to recover the classical size-independent shear modulus  $\mu^* \equiv \mu_{\text{macro}}$ . This imposes already some telling relations between the remaining parameters of the model.

Another interesting limit case concerns the shear stiffness for arbitrary “flat” samples ( $h \rightarrow 0$ ), which correspond to  $L_c \rightarrow \infty$ . Then, typically,  $\mu^*|_{L_c \rightarrow \infty}$  is an increasing function of  $L_c$ . Whether or not there exists an upper bound on the shear stiffness depends then on the specific model. Typically, gradient elasticity (including the indeterminate couple stress model) exhibits an unphysical stiffness singularity. Other more general models may have the same stiffness singularity in conjunction with the limit to infinity for further material parameters.

As a first result we can note that the simple shear of an infinite block is triggering an inhomogeneous solution when forced by the boundary condition, but this inhomogeneity remains for many of the investigated models “tame”, in the sense that the shear stiffness remains bounded as  $L_c \rightarrow \infty$  ( $h \rightarrow 0$ ). We expect this to change completely when we repeat this kind of investigation for the pure bending case in a future contribution.

Since we aim at a readable exposition, we use direct tensor notation alongside index-notation. Moreover, due to the large number of constitutive coefficients, especially in the curvature energies of the different models, we have opted to simplify the curvature expressions to a 1-parameter format for the classical micromorphic model, the microstrain model and the gradient elasticity model. For all other models, the effective curvature parameters are completely taken into account; nevertheless, they simplify considerably for the chosen 2D simple shear problem.

All our investigated generalized continuum models are in one way or another derived from the general Mindlin–Eringen [22] micromorphic framework. They differ in the choice of the additional independent degrees of freedom (Cosserat: 3 rotation dof, microstrain: 6 strain dof, etc.) besides the classical 3 translation degrees of freedom. They also differ in the choice of curvature parameters. The different curvature terms also presuppose according different boundary conditions, e.g., if the full gradient of the micro distortion  $\mathbf{P}$  is used as curvature (as in the classical micromorphic model)  $\|\nabla \mathbf{P}\|^2$ , then one can impose Dirichlet boundary conditions on  $\mathbf{P}$  completely. If, on the other hand, only the Curl of the micro distortion  $\mathbf{P}$  is controlled, as in the relaxed micromorphic model  $\|\text{Curl} \mathbf{P}\|^2$ , then only tangential boundary conditions on  $\mathbf{P}$  can be prescribed.

In second gradient elasticity, one controls  $\|\nabla^2 \mathbf{u}\|^2$  and accordingly, the values of  $\nabla \mathbf{u}$  at the boundary can be given, similarly for the indeterminate-couple stress model, in which  $\|\nabla \text{curl} \mathbf{u}\|^2$  is controlled and one may prescribe the values of  $\text{curl} \mathbf{u}$  at the boundary. For the Cosserat model, the curvature measure can be taken to be  $\|\text{Curl} \mathbf{A}\|^2$ , for a skew-symmetric matrix  $\mathbf{A}$ . Since Curl controls all first partial derivatives of  $\mathbf{A}$ , the tangential condition for skew-symmetric  $\mathbf{A}$  is equivalent to a full Dirichlet condition.

The apparent size-effect inherent in all these theories is strongly related to the employed Dirichlet boundary conditions for the additional (or higher order) terms. Indeed, if the additional degrees of freedom are left free at the upper and lower surface (for simple shear), then the solution turns into the homogeneous classical simple shear solution without size effects.

A long version of the paper, including all the technical details, can be found in [36].

### 1.1 Notation

For vectors  $\mathbf{a}, \mathbf{b} \in \mathbb{R}^n$ , we consider the scalar product  $\langle \mathbf{a}, \mathbf{b} \rangle := \sum_{i=1}^n a_i b_i \in \mathbb{R}$ , the (squared) norm  $\|\mathbf{a}\|^2 := \langle \mathbf{a}, \mathbf{a} \rangle$  and the dyadic product  $\mathbf{a} \otimes \mathbf{b} := (a_i b_j)_{i,j=1,\dots,n} \in \mathbb{R}^{n \times n}$ . Similarly, for tensors  $\mathbf{P}, \mathbf{Q} \in \mathbb{R}^{n \times n}$  with Cartesian coordinates  $P_{ij}$  and  $Q_{ij}$ , we define the scalar product  $\langle \mathbf{P}, \mathbf{Q} \rangle := \sum_{i,j=1}^n P_{ij} Q_{ij} \in \mathbb{R}$  and the (squared) Frobenius-norm  $\|\mathbf{P}\|^2 := \langle \mathbf{P}, \mathbf{P} \rangle$ . Moreover,  $\mathbf{P}^T := (P_{ji})_{i,j=1,\dots,n}$  denotes the transposition of the matrix  $\mathbf{P} = (P_{ij})_{i,j=1,\dots,n}$ , which decomposes orthogonally into the symmetric part  $\text{sym}\mathbf{P} := \frac{1}{2}(\mathbf{P} + \mathbf{P}^T)$  and the skew-symmetric part  $\text{skew}\mathbf{P} := \frac{1}{2}(\mathbf{P} - \mathbf{P}^T)$ . The Lie-Algebra of skew-symmetric matrices is denoted by  $\mathfrak{so}(3) := \{\mathbf{A} \in \mathbb{R}^{3 \times 3} \mid \mathbf{A}^T = -\mathbf{A}\}$ . The identity matrix is denoted by  $\mathbb{1}$ , so that the trace of a matrix  $\mathbf{P}$  is given by  $\text{tr}\mathbf{P} := \langle \mathbf{P}, \mathbb{1} \rangle$ . The gradient and the curl for a vector field  $\mathbf{u}$  are defined as

$$\nabla \mathbf{u} = \begin{pmatrix} u_{1,1} & u_{1,2} & u_{1,3} \\ u_{2,1} & u_{2,2} & u_{2,3} \\ u_{3,1} & u_{3,2} & u_{3,3} \end{pmatrix}, \quad \text{curl } \mathbf{u} = \nabla \times \mathbf{u} = \begin{pmatrix} u_{3,2} - u_{2,3} \\ u_{1,3} - u_{3,1} \\ u_{2,1} - u_{1,2} \end{pmatrix}. \quad (1)$$

Moreover, we introduce the Curl and the Div operators of the matrix  $\mathbf{P}$  as:

$$\text{Curl } \mathbf{P} = \begin{pmatrix} \text{curl}(P_{11}, P_{12}, P_{13}) \\ \text{curl}(P_{21}, P_{22}, P_{23}) \\ \text{curl}(P_{31}, P_{32}, P_{33}) \end{pmatrix}, \quad \text{Div } \mathbf{P} = \begin{pmatrix} \text{div}(P_{11}, P_{12}, P_{13}) \\ \text{div}(P_{21}, P_{22}, P_{23}) \\ \text{div}(P_{31}, P_{32}, P_{33}) \end{pmatrix}. \quad (2)$$

## 2 Simple shear for the isotropic Cauchy continuum

The expression of the strain energy for an isotropic Cauchy continuum is

$$W(\nabla \mathbf{u}) = \mu_{\text{macro}} \|\text{sym}\nabla \mathbf{u}\|^2 + \frac{\lambda_{\text{macro}}}{2} \text{tr}^2(\nabla \mathbf{u}), \quad (3)$$

while the equilibrium equations without body forces are

$$\text{Div} [2 \mu_{\text{macro}} \text{sym}\nabla \mathbf{u} + \lambda_{\text{macro}} \text{tr}(\nabla \mathbf{u}) \mathbb{1}] = \mathbf{0}. \quad (4)$$

The boundary conditions for the simple shear problem are  $u_1(x_2 = 0) = 0, u_1(x_2 = h) = \gamma h, u_2(x_2 = 0) = 0$ , and  $u_2(x_2 = h) = 0$  (see Fig. 1). The displacement fields solution and the shear stiffness for the simple shear problem are the following:

$$u_1(x_2) = \gamma x_2, \quad u_2(x_2) = 0, \quad \mu^* = \frac{\sigma_{12}}{\gamma} = \mu_{\text{macro}}. \quad (5)$$

Here and in the remainder of this work, the elastic coefficients  $\mu_i, \lambda_i$  are expressed in [MPa], the shear deformation  $\gamma$  is dimensionless, the lengths  $L_c$  and the thickness  $h$  in meter [m].

### 3 Classical Mindlin–Eringen formulation

The classical micromorphic model couples the displacement  $\mathbf{u} \in \mathbb{R}^3$  with an affine field  $\mathbf{P} \in \mathbb{R}^{3 \times 3}$ , called the micro-distortion. In the isotropic case, the elastic energy can be represented as

$$\begin{aligned}
 W(\nabla \mathbf{u}, \mathbf{P}, \nabla \mathbf{P}) &= \widehat{\mu} \|\text{sym } \nabla \mathbf{u}\|^2 + \frac{\widehat{\lambda}}{2} \text{tr}^2(\nabla \mathbf{u}) + \frac{b_1}{2} \text{tr}^2(\nabla \mathbf{u} - \mathbf{P}) \\
 &+ \frac{b_2}{2} \|\nabla \mathbf{u} - \mathbf{P}\|^2 + \frac{b_3}{2} \langle \nabla \mathbf{u} - \mathbf{P}, (\nabla \mathbf{u} - \mathbf{P})^T \rangle \\
 &+ g_1 \text{tr}(\nabla \mathbf{u}) \text{tr}(\nabla \mathbf{u} - \mathbf{P}) \\
 &+ g_2 \langle \text{sym } \nabla \mathbf{u}, (\nabla \mathbf{u} - \mathbf{P})^T \rangle + \frac{1}{2} \langle \mathbb{A} \nabla \mathbf{P}, \nabla \mathbf{P} \rangle \\
 &= \widehat{\mu} \epsilon_{ij} \epsilon_{ij} + \frac{\widehat{\lambda}}{2} \epsilon_{ii} \epsilon_{jj} + \frac{b_1}{2} \gamma_{ii} \gamma_{jj} + \frac{b_2}{2} \gamma_{ij} \gamma_{ij} + \frac{b_3}{2} \gamma_{ij} \gamma_{ji} \\
 &+ g_1 \gamma_{ii} \epsilon_{jj} + g_2 (\gamma_{ij} + \gamma_{ji}) \epsilon_{ij} + a_1 \chi_{iik} \chi_{kjj} + a_2 \chi_{iik} \chi_{jkj} \\
 &+ \frac{1}{2} a_3 \chi_{iik} \chi_{jjk} + \frac{1}{2} a_4 \chi_{ijj} \chi_{ikk} + a_5 \chi_{ijj} \chi_{kik} \\
 &+ \frac{1}{2} a_8 \chi_{iji} \chi_{kjk} + \frac{1}{2} a_{10} \chi_{ijk} \chi_{ijk} + a_{11} \chi_{ijk} \chi_{jki} \\
 &+ \frac{1}{2} a_{13} \chi_{ijk} \chi_{ikj} + \frac{1}{2} a_{14} \chi_{ijk} \chi_{jik} + \frac{1}{2} a_{15} \chi_{ijk} \chi_{kji}
 \end{aligned} \tag{6}$$

where  $\boldsymbol{\epsilon} = \text{sym } \nabla \mathbf{u}$  is the symmetric part of the gradient of the displacement field,  $\boldsymbol{\gamma} = \nabla \mathbf{u} - \mathbf{P}$  is the difference between the gradient of the displacement field and the micro-distortion tensor, and  $\chi_{ijk} = P_{jk,i}$  is the gradient of the micro-distortion.

To the authors knowledge, the only simple shear analytical solution available in the literature for this model is obtained for a very restrictive choice of parameters [15,41]<sup>1</sup>. In that specific case, the simple shear solution for the micro-distortion field  $\mathbf{P}$  obtains the format

$$\mathbf{P} = \begin{pmatrix} 0 & P_{12}(x_2) & 0 \\ 0 & 0 & 0 \\ 0 & 0 & 0 \end{pmatrix} \quad \text{and} \quad \nabla \mathbf{u} = \begin{pmatrix} 0 & u_{1,2}(x_2) & 0 \\ 0 & 0 & 0 \\ 0 & 0 & 0 \end{pmatrix}. \tag{7}$$

In general, such a format of the solution is not to be expected. While it is possible to construct the general simple shear solution to the classical micromorphic model Eq. (6), for comparison with our other models we consider the energy

$$\begin{aligned}
 W(\nabla \mathbf{u}, \mathbf{P}, \nabla \mathbf{P}) &= \frac{\mu_e + \mu_{\text{micro}} + \mu_c}{2} \|\nabla \mathbf{u} - \mathbf{P}\|^2 + \frac{\mu_e + \mu_{\text{micro}} - \mu_c}{2} \langle \nabla \mathbf{u} - \mathbf{P}, (\nabla \mathbf{u} - \mathbf{P})^T \rangle \\
 &+ \frac{\lambda_e + \lambda_{\text{micro}}}{2} \text{tr}^2(\nabla \mathbf{u} - \mathbf{P}) \\
 &+ \mu_{\text{micro}} \|\text{sym } \nabla \mathbf{u}\|^2 + \frac{\lambda_{\text{micro}}}{2} \text{tr}^2(\nabla \mathbf{u}) \\
 &- 2\mu_{\text{micro}} \langle \nabla \mathbf{u} - \mathbf{P}, \text{sym } \nabla \mathbf{u} \rangle \\
 &- \lambda_{\text{micro}} \text{tr}(\nabla \mathbf{u} - \mathbf{P}) \text{tr}(\nabla \mathbf{u}) + \frac{\mu L_c^2}{2} \|\nabla \mathbf{P}\|^2,
 \end{aligned} \tag{8}$$

being a special case of Eq. (6), by setting the values of the elastic parameters as follow (see [24])

$$\begin{aligned}
 \widehat{\mu} &= \mu_{\text{micro}}, \quad \widehat{\lambda} = \lambda_{\text{micro}}, \quad b_1 = \lambda_e + \lambda_{\text{micro}}, \\
 b_2 &= \mu_e + \mu_{\text{micro}} + \mu_c, \quad b_3 = \mu_e + \mu_{\text{micro}} - \mu_c, \\
 g_1 &= -\lambda_{\text{micro}}, \quad g_2 = -2\mu_{\text{micro}}, \quad a_{10} = \mu L_c^2, \\
 a_{\{1,2,3,4,5,8,11,13,14,15\}} &= 0.
 \end{aligned} \tag{9}$$

<sup>1</sup> The following energy expression has been used in [41]:  $W(\nabla \mathbf{u}, \mathbf{P}, \nabla \mathbf{P}) = \mu \|\text{sym } \nabla \mathbf{u}\|^2 + \lambda/2 \text{tr}^2(\nabla \mathbf{u}) + \alpha \mu \|\nabla \mathbf{u} - \mathbf{P}\|^2 + \alpha \lambda/2 \text{tr}^2(\nabla \mathbf{u} - \mathbf{P}) + \mu L_c^2/2 \|\nabla \mathbf{P}\|^2$ . This formulations is not reconcilable with the relaxed micromorphic model even if we neglect the curvature part.

We are going to show results for this model in its simplified form Eq. (8) in Sect. 8.

#### 4 Micro-void and micro-stretch model

The expression of the strain energy for the isotropic micro-void continuum with a single curvature parameter (3+1=4 dof's) can be written as:

$$\begin{aligned} W(\nabla \mathbf{u}, \omega, \text{Curl}(\omega \mathbb{1})) &= \mu_e \|\text{sym} \nabla \mathbf{u} - \omega \mathbb{1}\|^2 + \frac{\lambda_e}{2} \text{tr}^2(\nabla \mathbf{u} - \omega \mathbb{1}) + \mu_{\text{micro}} \|\omega \mathbb{1}\|^2 \\ &+ \frac{\lambda_{\text{micro}}}{2} \text{tr}^2(\omega \mathbb{1}) + \frac{\mu L_c^2}{2} \|\text{Curl}(\omega \mathbb{1})\|^2. \end{aligned} \quad (10)$$

Here,  $\omega : \mathbb{R}^3 \rightarrow \mathbb{R}$  describes the additional micro-voids degree of freedom. On the other hand the expression of the strain energy for the isotropic micro-stretch continuum with a single curvature parameter (3+3+1=7 dof's) can be written as [27]:

$$\begin{aligned} W(\nabla \mathbf{u}, \mathbf{A}, \omega, \text{Curl}(\mathbf{A} - \omega \mathbb{1})) &= \mu_e \|\text{sym} \nabla \mathbf{u} - \omega \mathbb{1}\|^2 + \frac{\lambda_e}{2} \text{tr}^2(\nabla \mathbf{u} - \omega \mathbb{1}) + \mu_c \|\text{skew}(\nabla \mathbf{u} - \mathbf{A})\|^2 \\ &+ \mu_{\text{micro}} \|\omega \mathbb{1}\|^2 + \frac{\lambda_{\text{micro}}}{2} \text{tr}^2(\omega \mathbb{1}) + \frac{\mu L_c^2}{2} \|\text{Curl}(\mathbf{A} + \omega \mathbb{1})\|^2, \end{aligned} \quad (11)$$

where  $\mathbf{A} \in \mathfrak{so}(3)$  and  $\omega \in \mathbb{R}$ . Both these micro-void and micro-stretch models can be obtained as special cases of the relaxed micromorphic model and because of that, the full solution is not reported in this work.

#### 5 Simple shear for the isotropic relaxed micromorphic model

The expression of the strain energy for the isotropic relaxed micromorphic continuum is:

$$\begin{aligned} W(\nabla \mathbf{u}, \mathbf{P}, \text{Curl} \mathbf{P}) &= \mu_e \|\text{sym}(\nabla \mathbf{u} - \mathbf{P})\|^2 + \frac{\lambda_e}{2} \text{tr}^2(\nabla \mathbf{u} - \mathbf{P}) \\ &+ \mu_c \|\text{skew}(\nabla \mathbf{u} - \mathbf{P})\|^2 + \mu_{\text{micro}} \|\text{sym} \mathbf{P}\|^2 \\ &+ \frac{\lambda_{\text{micro}}}{2} \text{tr}^2(\mathbf{P}) + \frac{\mu L_c^2}{2} \|\text{Curl} \mathbf{P}\|^2, \end{aligned} \quad (12)$$

while the equilibrium equations without body forces are the following:

$$\begin{aligned} \text{Div} \left[ \overbrace{2\mu_e \text{sym}(\nabla \mathbf{u} - \mathbf{P}) + \lambda_e \text{tr}(\nabla \mathbf{u} - \mathbf{P}) \mathbb{1} + 2\mu_c \text{skew}(\nabla \mathbf{u} - \mathbf{P})}^{\tilde{\sigma}} \right] &= \mathbf{0}, \\ \tilde{\sigma} - 2\mu_{\text{micro}} \text{sym} \mathbf{P} - \lambda_{\text{micro}} \text{tr}(\mathbf{P}) \mathbb{1} - \mu L_c^2 \text{Curl} \text{Curl} \mathbf{P} &= \mathbf{0}. \end{aligned} \quad (13)$$

Note that contrary to the full micromorphic model, the momentum stress tensor  $\mathbf{m} = \mu L_c^2 \text{Curl} \mathbf{P}$  remains of second order due to the Curl operator. It can be noted that  $\tilde{\sigma}$  can be obtained from Eq. (13)<sub>2</sub> and substituted into Eq. (13)<sub>1</sub>. This allows us to obtain the following relation

$$\text{Div} [2\mu_{\text{micro}} \text{sym} \mathbf{P} + \lambda_{\text{micro}} \text{tr}(\mathbf{P}) \mathbb{1}] = \mathbf{0}, \quad (14)$$

which can be seen as a classical elastic equilibrium equation at the micro-level. Due to the fact that the shear problem is point symmetric with respect to the center of the stripe, the following assumptions have been made on the structure of  $\mathbf{u}$  and  $\mathbf{P}$  (for the solution with no ansatz see [36]):

$$\mathbf{u} = \begin{pmatrix} u_1(x_2) \\ 0 \\ 0 \end{pmatrix}, \quad \mathbf{P} = \begin{pmatrix} 0 & P_{12}(x_2) & 0 \\ P_{21}(x_2) & 0 & 0 \\ 0 & 0 & 0 \end{pmatrix}. \quad (15)$$

The boundary conditions for the simple shear are the following:

$$u_1(x_2 = 0) = 0, \quad u_1(x_2 = h) = \gamma h, \quad P_{21}(x_2 = 0) = 0, \quad P_{21}(x_2 = h) = 0. \quad (16)$$

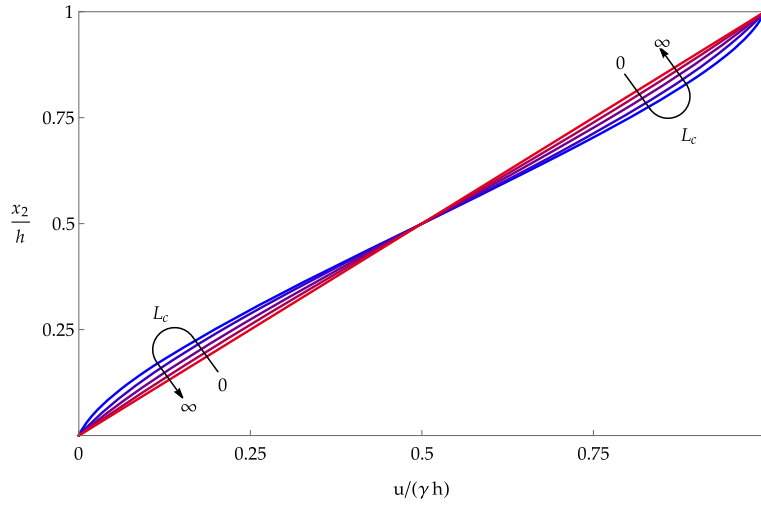


**Fig. 2** Profile of the dimensionless displacement field for the relaxed micromorphic model for  $f_1 = 1.117$ ,  $f_2 = 0.715$  and different values of  $L_c = \{0.4, 1.25, 2., 3.\bar{3}, 100\}$ . It is interesting to observe that there appears the maximal inhomogeneity in the displacement not for  $L_c \rightarrow \infty$  (also equivalent to  $h \rightarrow 0$ ) but at an intermediate value

The constraint on the components of  $\mathbf{P}$  is given by the compatibility condition  $\nabla \mathbf{u} \cdot \boldsymbol{\tau} = \mathbf{P} \cdot \boldsymbol{\tau}$ , where  $\boldsymbol{\tau}$  is the tangential unit vector on the upper and lower surface.

After substituting the expressions Eq. (15) in Eq. (13), the non-trivial equilibrium equations reduces to the following:

$$\begin{aligned}
 (\mu_e + \mu_c) P'_{12}(x_2) + (\mu_e - \mu_c) P'_{21}(x_2) - (\mu_e + \mu_c) u''_1(x_2) &= 0, \\
 (\mu_e + \mu_{\text{micro}} + \mu_c) P_{12}(x_2) + (\mu_e + \mu_{\text{micro}} - \mu_c) P_{21}(x_2) - (\mu_c + \mu_e) u'_1(x_2) &= 0, \\
 (\mu_e + \mu_{\text{micro}} - \mu_c) P_{12}(x_2) + (\mu_e + \mu_{\text{micro}} + \mu_c) P_{21}(x_2) - (\mu_e - \mu_c) u'_1(x_2) - \mu L_c^2 P''_{21}(x_2) &= 0.
 \end{aligned}
 \tag{17}$$

After applying the boundary conditions Eq. (16), the expressions of the nonzero components of the displacement and micro-distortion fields result to be:

$$\begin{aligned}
 u_1(x_2) &= \frac{\frac{f_2 L_c}{h} \sinh\left(\frac{f_1(h-2x_2)}{L_c}\right) + \frac{2x_2}{h} \cosh\left(\frac{f_1 h}{L_c}\right) - \frac{f_2 L_c}{h} \sinh\left(\frac{f_1 h}{L_c}\right)}{\cosh\left(\frac{f_1 h}{L_c}\right) - \frac{f_2 L_c}{h} \sinh\left(\frac{f_1 h}{L_c}\right)} \frac{\gamma h}{2}, \\
 P_{21}(x_2) &= -\frac{\sinh\left(\frac{f_1 x_2}{L_c}\right) \sinh\left(\frac{f_1(h-x_2)}{L_c}\right)}{\cosh\left(\frac{f_1 h}{L_c}\right) - \frac{f_2 L_c}{h} \sinh\left(\frac{f_1 h}{L_c}\right)} \frac{\mu_{\text{micro}}}{\mu_e + \mu_{\text{micro}}} \gamma, \\
 P_{12}(x_2) &= \frac{\cosh\left(\frac{f_1 h}{L_c}\right) \mu_e + \sinh\left(\frac{f_1 x_2}{L_c}\right) \sinh\left(\frac{f_1(h-x_2)}{L_c}\right) \mu_{\text{micro}}}{\cosh\left(\frac{f_1 h}{L_c}\right) - \frac{f_2 L_c}{h} \sinh\left(\frac{f_1 h}{L_c}\right)} \frac{1}{\mu_e + \mu_{\text{micro}}} \gamma, \\
 f_1 &:= \sqrt{\frac{\mu_c \mu_e}{\mu(\mu_c + \mu_e)}} \quad f_2 := \frac{1}{f_1} \frac{\mu_c \mu_{\text{micro}}}{(\mu_c + \mu_e)(\mu_e + \mu_{\text{micro}})}.
 \end{aligned}
 \tag{18}$$

A plot of the displacement field while varying  $L_c$  is shown in Fig. 2.

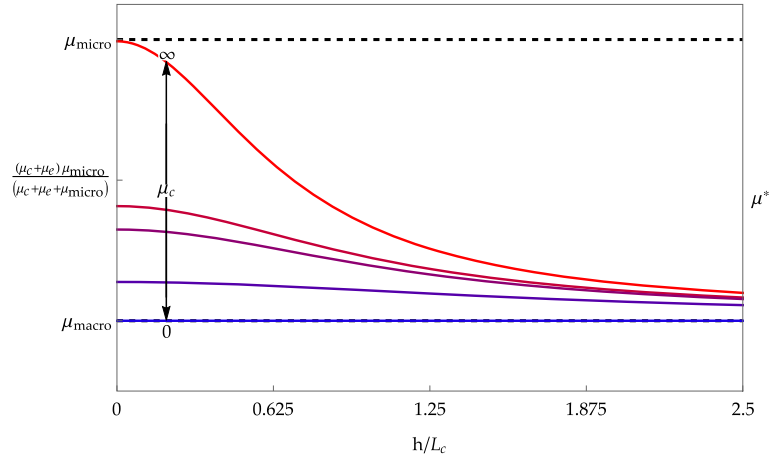


**Fig. 3** The apparent shear stiffness  $\mu^*$  governed by  $\mu_{\text{macro}}$  (for  $L_c = 0$ ) and  $\frac{(\mu_c + \mu_e)\mu_{\text{micro}}}{\mu_c + \mu_e + \mu_{\text{micro}}}$  (for  $L_c \rightarrow \infty$ ). In all possible limit cases (except  $\mu_{\text{micro}} \rightarrow \infty$ ) the relaxed micromorphic model has bounded shear stiffness. The maximum possible shear stiffness is given by  $\mu_{\text{micro}}$ . The values of the elastic parameters that have been used are:  $\mu = 1$ ,  $\mu_e = 1.25$ ,  $\mu_{\text{micro}} = 5$ , and  $\mu_c = \{1000, 4.3, 3, 1, 0.00001\}$

It is worth to be highlighted that  $\text{sym } \mathbf{P}$  results to be constant, which satisfies trivially Eq. (14). The following relation is a measure of the apparent shear stiffness (see Fig. 3)

$$\mu^* = \frac{\tilde{\sigma}_{12}}{\gamma} = \frac{1}{1 - \frac{f_2 L_c}{h} \tanh\left(\frac{f_1 h}{L_c}\right)} \frac{\mu_e \mu_{\text{micro}}}{\mu_e + \mu_{\text{micro}}}. \quad (19)$$

## 6 Simple shear for the isotropic Cosserat continuum

The expression of the strain energy for the Cosserat continuum can be written as:

$$W(\nabla \mathbf{u}, \mathbf{A}, \text{Curl } \mathbf{A}) = \mu_e \|\text{sym } \nabla \mathbf{u}\|^2 + \frac{\lambda_e}{2} \text{tr}^2(\nabla \mathbf{u}) + \mu_c \|\text{skew}(\nabla \mathbf{u} - \mathbf{A})\|^2 + \frac{\mu L_c^2}{2} \|\text{Curl } \mathbf{A}\|^2, \quad (20)$$

where  $\mathbf{A} \in \mathfrak{so}(3)$ . The equilibrium equations without body forces are the following:

$$\text{Div} \left[ \overbrace{2\mu_e \text{sym } \nabla \mathbf{u} + \lambda_e \text{tr}(\nabla \mathbf{u}) \mathbb{1} + 2\mu_c \text{skew}(\nabla \mathbf{u} - \mathbf{A})}^{\tilde{\boldsymbol{\sigma}}} \right] = \mathbf{0}, \quad (21)$$

$$2\mu_c \text{skew}(\nabla \mathbf{u} - \mathbf{A}) - \mu L_c^2 \text{skew } \text{Curl } \text{Curl } \mathbf{A} = \mathbf{0}.$$

This model is a special limit case of the relaxed micromorphic model for  $\mu_{\text{micro}} \rightarrow \infty$ .

Due to the symmetry of the shear problem the following assumptions are made on the structure of  $\mathbf{u}$  and  $\mathbf{A}$ :

$$\mathbf{u} = \begin{pmatrix} u_1(x_2) \\ 0 \\ 0 \end{pmatrix}, \quad \mathbf{A} = \begin{pmatrix} 0 & A_{21}(x_2) & 0 \\ -A_{21}(x_2) & 0 & 0 \\ 0 & 0 & 0 \end{pmatrix}. \quad (22)$$

The boundary conditions for the simple shear are the following:

$$u_1(x_2 = 0) = 0, \quad u_1(x_2 = h) = \gamma h, \quad A_{21}(x_2 = 0) = 0, \quad A_{21}(x_2 = h) = 0 \quad (23)$$

The constraint on the components of  $\mathbf{A}$  are given by the compatibility condition  $\nabla \mathbf{u} \cdot \boldsymbol{\tau} = \mathbf{A} \cdot \boldsymbol{\tau}$ , where  $\boldsymbol{\tau}$  is the tangential unit vector on the upper and lower surface. The resulting combination constrains  $\mathbf{A}$  to be zero at the upper and lower surface.

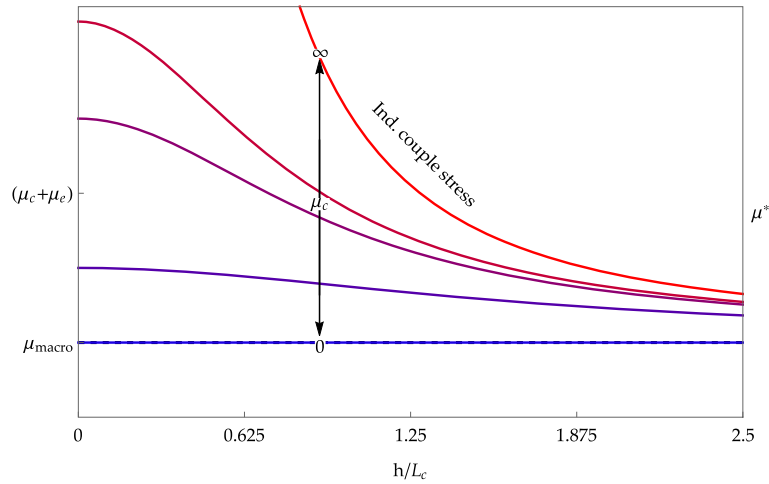


**Fig. 4** The Cosserat model and its shear stiffness response  $\mu^*$  as a function of  $L_c$ . For  $0 < \mu_c < \infty$  we observe bounded shear stiffness, for all values of the characteristic size  $L_c$ . For  $\mu_c \rightarrow \infty$  the solution of the indeterminate couple stress model is retrieved for which the shear stiffness is singular for  $L_c \rightarrow \infty$  ( $h \rightarrow 0$ ) due to the applied boundary conditions. Also,  $\mu_e \rightarrow \infty$  generate a singularity for  $L_c \rightarrow \infty$ . The values of the elastic parameters that have been used are:  $\mu = 1$ ,  $\mu_e = 1.25$ , and  $\mu_c = \{1000, 4.3, 3, 1, 0.00001\}$

After substituting the expressions Eq. (22) in Eq. (21), the non-trivial equilibrium equations reduces to the following (for the solution with no ansatz see [36]):

$$\begin{aligned}
 (\mu_c + \mu_e) u_1''(x_2) - 2 \mu_c A_{21}'(x_2) &= 0, \\
 \frac{1}{2} \mu L_c^2 A_{21}''(x_2) - 2 \mu_c A_{21}(x_2) + \mu_c u_1'(x_2) &= 0.
 \end{aligned}
 \tag{24}$$

After applying the boundary conditions Eq. (23), the expressions of the nonzero components of the displacement and micro-distortion fields result to be (see also [14, 30]):

$$\begin{aligned}
 u_1(x_2) &= \frac{\tilde{f}_2 L_c \sinh\left(\frac{f_1(h-2x_2)}{L_c}\right) + \frac{2x_2}{h} \cosh\left(\frac{f_1 h}{L_c}\right) - \frac{\tilde{f}_2 L_c}{h} \sinh\left(\frac{f_1 h}{L_c}\right)}{\cosh\left(\frac{f_1 h}{L_c}\right) - \frac{\tilde{f}_2 L_c}{h} \sinh\left(\frac{f_1 h}{L_c}\right)} \frac{\gamma h}{2}, \\
 A_{21}(x_2) &= -\frac{\sinh\left(\frac{f_1 x_2}{L_c}\right) \sinh\left(\frac{f_1(h-x_2)}{L_c}\right)}{\cosh\left(\frac{f_1 h}{L_c}\right) - \frac{\tilde{f}_2 L_c}{h} \sinh\left(\frac{f_1 h}{L_c}\right)} \gamma, \\
 f_1 &= \sqrt{\frac{\mu_c \mu_e}{\mu(\mu_c + \mu_e)}}, \\
 \tilde{f}_2 &= \frac{1}{f_1} \frac{\mu_c}{\mu_e + \mu_c}.
 \end{aligned}
 \tag{25}$$

The following relation is a measure of the higher-order stiffness (see Fig. 4)

$$\mu^* = \frac{1}{1 - \frac{\tilde{f}_2 L_c}{h} \tanh\left(\frac{f_1 h}{L_c}\right)} \mu_e.
 \tag{26}$$



### 7 Simple shear for the isotropic indeterminate couple stress continuum

From the Cosserat model, we obtain the indeterminate couple stress model by constraining  $\mathbf{A} = \text{skew} \nabla \mathbf{u}$ . The expression of the strain energy for the indeterminate couple stress continuum is:

$$W(\nabla \mathbf{u}, \text{Curl skew} \nabla \mathbf{u}) = \mu_e \|\text{sym} \nabla \mathbf{u}\|^2 + \frac{\lambda_e}{2} \text{tr}^2(\nabla \mathbf{u}) + \frac{\mu L_c^2}{2} \|\text{Curl skew} \nabla \mathbf{u}\|^2, \tag{27}$$

while the equilibrium equations without body forces are the following:

$$\text{Div} [2\mu_e \text{sym} \nabla \mathbf{u} + \lambda_e \text{tr}(\nabla \mathbf{u}) \mathbb{1} + \mu L_c^2 \text{skew Curl Curl skew} \nabla \mathbf{u}] = \mathbf{0}. \tag{28}$$

This model is a special limit case of the Cosserat model for Cosserat couple modulus  $\mu_c \rightarrow \infty$ .

Due to the shear problem symmetry the following structure of  $\mathbf{u} = (u_1(x_2), 0, 0)^T$  has been chosen (for the solution with no ansatz see [36]). The boundary conditions for the simple shear are the following:

$$\begin{aligned} u_1(x_2 = 0) &= 0, & u_1(x_2 = h) &= \gamma h, \\ u_1'(x_2 = 0) &= 0, & u_1'(x_2 = h) &= 0. \end{aligned} \tag{29}$$

The constraint on the components of  $\nabla \mathbf{u}$  are given by the compatibility condition  $\text{skew} \nabla \mathbf{u} \cdot \boldsymbol{\tau} = \mathbf{0}$ , where  $\boldsymbol{\tau}$  is the tangential unit vector on the upper and lower surface.

After substituting the displacement field in Eq. (28), the non-trivial equilibrium equation reduces to the following

$$\mu_e u_1''(x_2) - \frac{1}{4} \mu L_c^2 u_1^{(4)}(x_2) = 0. \tag{30}$$

After applying the boundary conditions Eq. (29), the expression of the nonzero component of the displacement field results to be:

$$\begin{aligned} u_1(x_2) &= \frac{\frac{L_c}{\bar{f}_1 h} \sinh\left(\frac{\bar{f}_1(h-2x_2)}{L_c}\right) + \frac{2x_2}{h} \cosh\left(\frac{\bar{f}_1 h}{L_c}\right) - \frac{L_c}{\bar{f}_1 h} \sinh\left(\frac{\bar{f}_1 h}{L_c}\right)}{\cosh\left(\frac{\bar{f}_1 h}{L_c}\right) - \frac{L_c}{\bar{f}_1 h} \sinh\left(\frac{\bar{f}_1 h}{L_c}\right)} \frac{\gamma h}{2}, \\ \bar{f}_1 &:= \sqrt{\frac{\mu_e}{\mu}}. \end{aligned} \tag{31}$$

The following relation is a measure of the higher-order stiffness, and it can be seen in Fig. 4

$$\mu^* = \frac{1}{1 - \frac{L_c}{\bar{f}_1 h} \tanh\left(\frac{\bar{f}_1 h}{L_c}\right)} \mu_e. \tag{32}$$

#### 7.1 Simple shear for the isotropic symmetric couple stress continuum

The expression of the strain energy for the isotropic symmetric couple stress continuum is:

$$W(\nabla \mathbf{u}, \text{Curl sym} \nabla \mathbf{u}) = \mu_e \|\text{sym} \nabla \mathbf{u}\|^2 + \frac{\lambda_e}{2} \text{tr}^2(\nabla \mathbf{u}) + \frac{\mu L_c^2}{2} \|\text{Curl sym} \nabla \mathbf{u}\|^2, \tag{33}$$

while the equilibrium equations without body forces are the following:

$$\text{Div} [2\mu_e \text{sym} \nabla \mathbf{u} + \lambda_e \text{tr}(\nabla \mathbf{u}) \mathbb{1} + \mu L_c^2 \text{sym Curl Curl sym} \nabla \mathbf{u}] = \mathbf{0}. \tag{34}$$

As it is shown in the appendix of [36],  $\text{Curl sym} \nabla \mathbf{u} = -\text{Curl skew} \nabla \mathbf{u}$ , which implies that the energy for this model, Eq. (33), is the same as the indeterminate couple stress continuum energy Eq. (27).

Furthermore, these two models share the same equilibrium equations (Eqs. (28) and (34)) since it is possible to prove that  $\text{Div} [\text{sym Curl Curl sym } \nabla \mathbf{u}] = \text{Div} [\text{skew Curl Curl skew } \nabla \mathbf{u}]$ .

The following expressions show how, in general, the boundary conditions of the symmetric couple stress continuum model ( $\text{sym } \nabla \mathbf{u} \cdot \boldsymbol{\tau} = \mathbf{0}$ ) differ from the ones for the indeterminate couple stress model ( $\text{skew } \nabla \mathbf{u} \cdot \boldsymbol{\tau} = \mathbf{0}$ ):

$$\text{sym } \nabla \mathbf{u} \cdot \boldsymbol{\tau} = \frac{1}{2} \begin{pmatrix} 2u_{1,1} \\ u_{1,2} + u_{2,1} \\ u_{1,3} + u_{3,1} \end{pmatrix}, \quad \text{skew } \nabla \mathbf{u} \cdot \boldsymbol{\tau} = \frac{1}{2} \begin{pmatrix} 0 \\ u_{2,1} - u_{1,2} \\ u_{3,1} - u_{1,3} \end{pmatrix}. \tag{35}$$

However, for the simple shear problem, since  $u_2 = 0$  and the displacement field does not depend on the coordinate  $x_1$ , Eqs. (35)<sub>1</sub> and (35)<sub>2</sub> end up to be the same:

$$\text{sym } \nabla \mathbf{u} \cdot \boldsymbol{\tau} = -\text{sym } \nabla \mathbf{u} \cdot \boldsymbol{\tau} = \left(0, \frac{u_{1,2}}{2}, 0\right)^T, \tag{36}$$

making this model completely equivalent to the indeterminate couple stress model for the simple shear problem.

Observe as well that Eq. (33) can be seen as a degenerate case of Mindlin’s strain gradient continuum Eq. (53) (Form I of [22]).

### 7.2 Simple shear for the isotropic modified couple stress continuum and for the isotropic “pseudo-consistent” couple stress continuum

The expression of the strain energy for the isotropic modified couple stress continuum is:

$$W(\nabla \mathbf{u}, \text{Curl skew } \nabla \mathbf{u}) = \mu_e \|\text{sym } \nabla \mathbf{u}\|^2 + \frac{\lambda_e}{2} \text{tr}^2(\nabla \mathbf{u}) + \frac{\mu \overline{L_c}^2}{2} \|\text{sym Curl skew } \nabla \mathbf{u}\|^2. \tag{37}$$

This energy is equivalent to the one of the isotropic indeterminate couple stress continuum beside a constant multiplying the curvature term (expressed via the different notation for length-scale parameter  $\overline{L_c}$ ) and this can be seen thanks to the calculation reported in the appendix of [36].

The expression of the strain energy for the “pseudo-consistent” couple stress continuum is [12,31]:

$$W(\nabla \mathbf{u}, \text{Curl skew } \nabla \mathbf{u}) = \mu_e \|\text{sym } \nabla \mathbf{u}\|^2 + \frac{\lambda_e}{2} \text{tr}^2(\nabla \mathbf{u}) + \frac{\mu \overline{L_c}^2}{2} \|\text{skew Curl skew } \nabla \mathbf{u}\|^2. \tag{38}$$

The authors of [31] have argued that the curvature term in the couple stress model should only depend on  $\|\text{skew Curl skew } \nabla \mathbf{u}\|$ . In appendix of [36], it is possible to see that for simple shear, the solution coincides with the modified couple stress model and the indeterminate couple stress model. Differences are expected to appear for other boundary value problems like bending.

## 8 Simple shear for the classical isotropic micromorphic continuum without mixed terms

The expression of the strain energy for the classical isotropic micromorphic continuum without mixed terms (like  $\langle \text{sym } \mathbf{P}, \text{sym}(\nabla \mathbf{u} - \mathbf{P}) \rangle$ , etc.) can be written as:

$$\begin{aligned} W(\nabla \mathbf{u}, \mathbf{P}, \nabla \mathbf{P}) = & \mu_e \|\text{sym}(\nabla \mathbf{u} - \mathbf{P})\|^2 + \frac{\lambda_e}{2} \text{tr}^2(\nabla \mathbf{u} - \mathbf{P}) + \mu_c \|\text{skew}(\nabla \mathbf{u} - \mathbf{P})\|^2 \\ & + \mu_{\text{micro}} \|\text{sym } \mathbf{P}\|^2 + \frac{\lambda_{\text{micro}}}{2} \text{tr}^2(\mathbf{P}) + \frac{\mu L_c^2}{2} \|\nabla \mathbf{P}\|^2, \end{aligned} \tag{39}$$

while the equilibrium equations without body forces are the following:

$$\begin{aligned} \text{Div} \left[ \overbrace{2\mu_e \text{sym}(\nabla \mathbf{u} - \mathbf{P}) + \lambda_e \text{tr}(\nabla \mathbf{u} - \mathbf{P}) \mathbb{1} + 2\mu_c \text{skew}(\nabla \mathbf{u} - \mathbf{P})}^{\tilde{\boldsymbol{\sigma}}} \right] = \mathbf{0}, \\ \tilde{\boldsymbol{\sigma}} - 2\mu_{\text{micro}} \text{sym } \mathbf{P} - \lambda_{\text{micro}} \text{tr}(\mathbf{P}) \mathbb{1} + \mu L_c^2 \text{Div} [\nabla \mathbf{P}] = \mathbf{0}. \end{aligned} \tag{40}$$

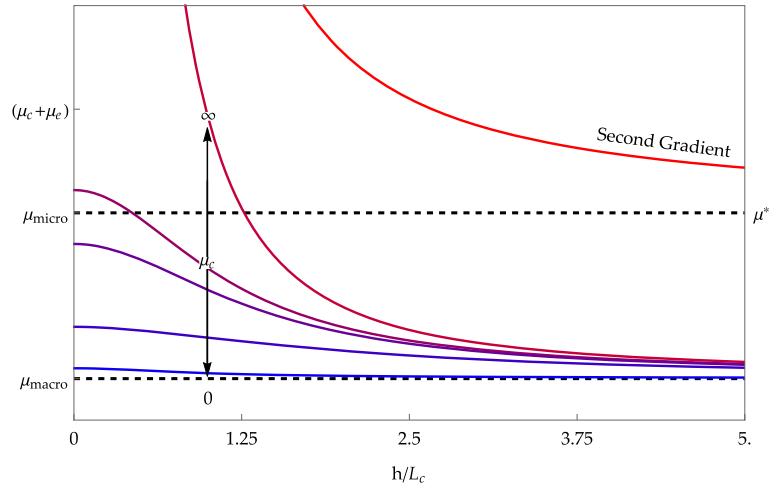


**Fig. 5** The classical micromorphic model without mixed terms. Plot of the shear stiffness as a function of  $L_c$ . For small  $L_c$  ( $h \rightarrow \infty$ ), the shear stiffness is given by  $\mu_{\text{macro}}$ , where  $\mu_{\text{macro}} = \frac{\mu_{\text{micro}} \mu_e}{\mu_{\text{micro}} + \mu_e}$ . For large  $L_c$  ( $h \rightarrow 0$ ), the shear stiffness is given by  $\mu_e + \mu_c$ . If either  $\mu_e$  or  $\mu_c \rightarrow \infty$ , there is a singularity appearing in the shear stiffness for  $L_c \rightarrow \infty$  ( $h \rightarrow 0$ ). The values of the elastic parameters that have been used are:  $\mu = 1$ ,  $\mu_e = 1.25$ ,  $\mu_{\text{micro}} = 5$ , and  $\mu_c = \{1000, 4.3, 3, 1, 0.00001\}$

Observe that the momentum stress tensor  $\mathbf{m} = \mu L_c^2 \nabla \mathbf{P}$  is of third order. The following assumptions are made on the structure of  $\mathbf{u}$  and  $\mathbf{P}$  due to the symmetry of the shear problem (for the solution with no ansatz see [36]):

$$\mathbf{u} = \begin{pmatrix} u_1(x_2) \\ 0 \\ 0 \end{pmatrix}, \quad \mathbf{P} = \begin{pmatrix} 0 & P_{12}(x_2) & 0 \\ P_{21}(x_2) & 0 & 0 \\ 0 & 0 & 0 \end{pmatrix}. \quad (41)$$

The boundary conditions for the simple shear are the following:

$$u_1(x_2 = 0) = 0, \quad u_1(x_2 = h) = \gamma h, \quad \mathbf{P}(x_2 = 0) = 0, \quad \mathbf{P}(x_2 = h) = 0. \quad (42)$$

It is important to underline that the constraint is applied on all the components of  $\mathbf{P}$  at the upper and lower surface. After substituting the expressions Eq. (41) in Eq. (40), the non-trivial equilibrium equations reduces to the following:

$$\begin{aligned} (\mu_e + \mu_c) P'_{12}(x_2) + (\mu_e - \mu_c) P'_{21}(x_2) - (\mu_e + \mu_c) u''_1(x_2) &= 0, \\ (\mu_e + \mu_{\text{micro}} + \mu_c) P_{12}(x_2) + (\mu_e + \mu_{\text{micro}} - \mu_c) P_{21}(x_2) - (\mu_c + \mu_e) u'_1(x_2) - \mu L_c^2 P''_{12}(x_2) &= 0, \\ (\mu_e + \mu_{\text{micro}} - \mu_c) P_{12}(x_2) + (\mu_e + \mu_{\text{micro}} + \mu_c) P_{21}(x_2) - (\mu_e - \mu_c) u'_1(x_2) - \mu L_c^2 P''_{21}(x_2) &= 0. \end{aligned} \quad (43)$$

After applying the boundary conditions Eq. (42), it is possible to obtain the analytical solution which unfortunately is too complicated to be reported here (see [36] for further details). Nevertheless, it is possible to plot how the apparent stiffness behaves while changing  $\mu_c$  and  $L_c$  (see Fig. 5)

## 9 Simple shear for Forest's micro-strain model with mixed terms

The micro-strain model considers a symmetric micro-distortion  $\mathbf{P} = \mathbf{S} \in \text{Sym}(3)$  and mixed terms like  $\langle \mathbf{S}, \text{sym} \nabla \mathbf{u} - \mathbf{S} \rangle$ , etc. The expression of the isotropic strain energy for Forest's micro-strain continuum [11, 15] with  $(3+6=9)$  degrees of freedom but with just one elastic curvature parameter is:

$$\begin{aligned} W(\nabla \mathbf{u}, \mathbf{S}, \nabla \mathbf{S}) &= \mu_e \|\text{sym} \nabla \mathbf{u} - \mathbf{S}\|^2 + \frac{\lambda_e}{2} \text{tr}^2(\nabla \mathbf{u} - \mathbf{S}) + \mu_{\text{micro}} \|\mathbf{S}\|^2 \\ &+ \frac{\lambda_{\text{micro}}}{2} \text{tr}^2(\mathbf{S}) + 2\mu_{\text{mix}} \langle \mathbf{S}, \text{sym} \nabla \mathbf{u} - \mathbf{S} \rangle \\ &+ \lambda_{\text{mix}} \text{tr}(\mathbf{S}) \text{tr}(\nabla \mathbf{u} - \mathbf{S}) + \frac{\mu L_c^2}{2} \|\nabla \mathbf{S}\|^2, \end{aligned} \quad (44)$$

where  $\mathbf{S} \in \text{Sym}(3)$ . The equilibrium equations without body forces are the following:

$$\overbrace{\text{Div} \left[ 2\mu_e (\text{sym} \nabla \mathbf{u} - \mathbf{S}) + \lambda_e \text{tr}(\nabla \mathbf{u} - \mathbf{S}) \mathbb{1} + 2\mu_{\text{mixed}} \mathbf{S} + \lambda_{\text{mixed}} \text{tr}(\mathbf{S}) \mathbb{1} \right]}^{\tilde{\sigma}} = \mathbf{0}, \quad (45)$$

$$2\mu_e (\text{sym} \nabla \mathbf{u} - \mathbf{S}) + \lambda_e \text{tr}(\nabla \mathbf{u} - \mathbf{S}) \mathbb{1} - 2(\mu_{\text{micro}} - 2\mu_{\text{mixed}}) \mathbf{S} - (\lambda_{\text{micro}} - 2\lambda_{\text{mixed}}) \text{tr}(\mathbf{S}) \mathbb{1} - 2\mu_{\text{mixed}} \text{sym} \nabla \mathbf{u} - \lambda_{\text{mixed}} \text{tr}(\nabla \mathbf{u}) \mathbb{1} + \mu L_c^2 \text{Div} [\nabla \mathbf{S}] = \mathbf{0}.$$

It is worth noticing the relation of this model to the relaxed micromorphic models: The curvature measure is based on  $\nabla \text{sym} \mathbf{P}$  instead of  $\text{Curl} \mathbf{P}$ ,  $\mu_c \equiv 0$  and the relaxed micromorphic model does not feature mixed terms. Such a model has also been proposed by [38] under the name ‘‘reduced micromorphic model’’ (‘‘RMM’’) [38]. It is also worth to highlight that, for the simple shear, the positive definiteness of the material is guaranteed when the following relations hold

$$\mu_e > 0, \quad \mu_{\text{micro}} > 0, \quad \mu_{\text{mix}}^2 < \mu_e \mu_{\text{micro}}. \quad (46)$$

Due to the shear problem symmetry, the structure of  $\mathbf{u}$  and  $\mathbf{S}$  has been chosen as follow (for the solution with no ansatz see [36]):

$$\mathbf{u} = \begin{pmatrix} u_1(x_2) \\ 0 \\ 0 \end{pmatrix}, \quad \mathbf{S} = \begin{pmatrix} 0 & S_{12}(x_2) & 0 \\ S_{12}(x_2) & 0 & 0 \\ 0 & 0 & 0 \end{pmatrix}. \quad (47)$$

The boundary conditions for the simple shear are the following:

$$u_1(x_2 = 0) = 0, \quad u_1(x_2 = h) = \gamma h, \quad S_{12}(x_2 = 0) = 0, \quad S_{12}(x_2 = h) = 0. \quad (48)$$

It is important to underline that the constraint is, in general, on all the components of  $\mathbf{S}$ .

After substituting the expressions Eq. (47) in Eq. (45), the non-trivial equilibrium equations reduces to the following:

$$2(\mu_{\text{mix}} - \mu_e) S'_{12}(x_2) + \mu_e u_1''(x_2) = 0, \quad (49)$$

$$2(\mu_e + \mu_{\text{micro}} - 2\mu_{\text{mix}}) S_{12}(x_2) - (\mu_e - \mu_{\text{mix}}) u_1'(x_2) - \mu L_c^2 S''_{12}(x_2) = 0,$$

After applying the boundary conditions Eq. (48), the solution of Eq. (49) for  $u_1(x_2)$  and  $S_{12}(x_2)$  is the following:

$$u_1(x_2) = \frac{\frac{f_3 L_c}{f_1 h} \left( \sinh \left( \frac{f_1 (h - 2x_2)}{2L_c} \right) - \sinh \left( \frac{f_1 h}{2L_c} \right) \right) + \frac{x_2}{h} \cosh \left( \frac{f_1 h}{2L_c} \right)}{\cosh \left( \frac{f_1 h}{2L_c} \right) - \frac{2f_3 L_c}{f_1 h} \sinh \left( \frac{f_1 h}{2L_c} \right)} \gamma h,$$

$$S_{12}(x_2) = \frac{\cosh \left( \frac{f_1 h}{2L_c} \right) - \cosh \left( \frac{f_1 (h - 2x_2)}{2L_c} \right)}{2 \cosh \left( \frac{f_1 h}{2L_c} \right) - \frac{4f_3 L_c}{f_1 h} \sinh \left( \frac{f_1 h}{2L_c} \right)} \frac{\mu_e - \mu_{\text{mix}}}{\mu_e + \mu_{\text{micro}} - 2\mu_{\text{mix}}} \gamma, \quad (50)$$

$$f_1 := \sqrt{\frac{2(\mu_e \mu_{\text{micro}} - \mu_{\text{mix}}^2)}{\mu_e \mu_e}},$$

$$f_3 := \frac{(\mu_e - \mu_{\text{mix}})^2}{\mu_e (\mu_e + \mu_{\text{micro}} - 2\mu_{\text{mix}})}.$$

The following relation is a measure of the higher-order stiffness (see Fig. 6)

$$\mu^* = \frac{1}{1 - \frac{2f_3 L_c}{f_1 h} \tanh \left( \frac{f_1 h}{2L_c} \right)} \frac{\mu_e \mu_{\text{micro}} - \mu_{\text{mix}}^2}{\mu_e + \mu_{\text{micro}} - 2\mu_{\text{mix}}}. \quad (51)$$

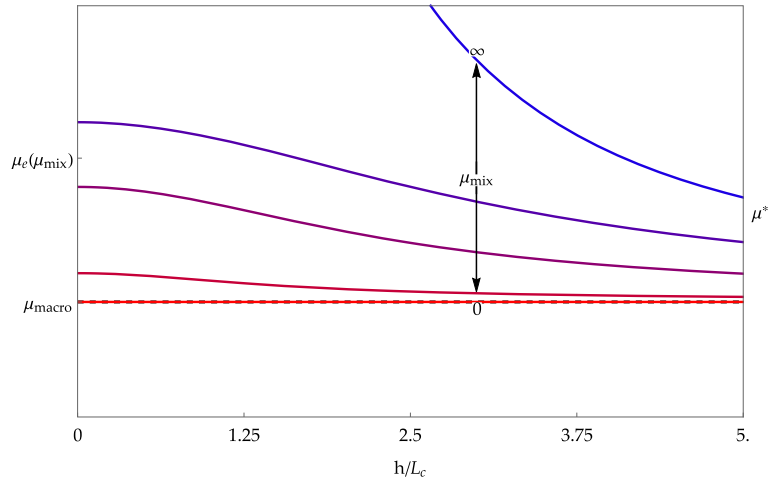


**Fig. 6** The size-dependent shear stiffness  $\mu^*$  for Forest’s micro-strain model. The values of the elastic parameters that have been used are:  $\mu = 1$ ,  $\mu_e = \{1, 1.25, 2, 2.56, 21.25\}$ ,  $\mu_{\text{micro}} = 5$ , and  $\mu_{\text{mix}} = \{1, 2, 3, 3.5, 10\}$

Since the limit  $\mu^*|_{L_c \rightarrow 0} = \frac{\mu_e \mu_{\text{micro}} - \mu_{\text{mix}}^2}{\mu_e + \mu_{\text{micro}} - 2\mu_{\text{mix}}} = \mu_{\text{macro}}$  (for  $\mu_{\text{mix}} = 0$  the classic value is retrieved) it is possible to evaluate  $\mu_e$  with respect to the other constant:

$$\mu_e = \frac{\mu_{\text{micro}} \mu_{\text{macro}} - 2\mu_{\text{macro}} \mu_{\text{mix}} + \mu_{\text{mix}}^2}{\mu_{\text{micro}} - \mu_{\text{macro}}}. \tag{52}$$

If  $\mu_{\text{macro}}$  is finite, if  $\mu_{\text{mix}} \rightarrow \infty$  we then have  $\mu_e \rightarrow \infty$  too. It is possible to decide to keep  $\mu_e$  finite, but this will imply that if  $\mu_{\text{mix}} \rightarrow \infty$ , then  $\mu_{\text{macro}} \rightarrow \infty$  too, which is not desirable.

**10 Simple shear for the second gradient continuum**

The expression of the strain energy for the isotropic second gradient continuum is:

$$W(\nabla \mathbf{u}, \nabla^2 \mathbf{u}) = \mu_{\text{micro}} \|\text{sym } \nabla \mathbf{u}\|^2 + \frac{\lambda_{\text{micro}}}{2} \text{tr}^2(\nabla \mathbf{u}) + \frac{\mu L_c^2}{2} \|\nabla^2 \mathbf{u}\|^2, \tag{53}$$

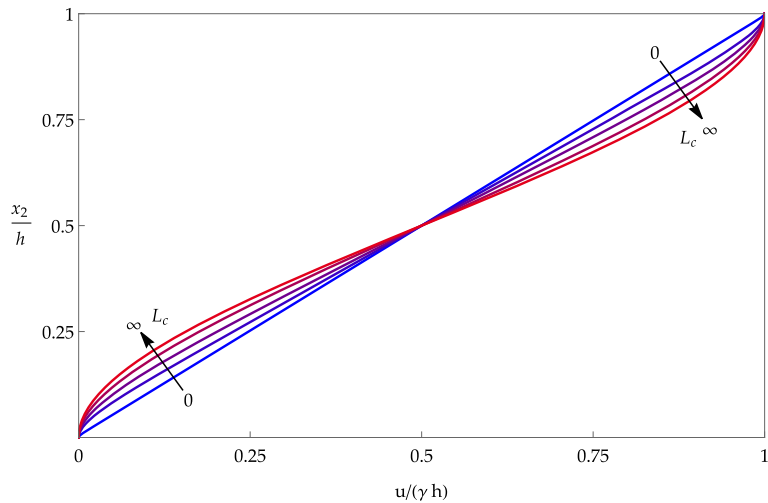


**Fig. 7** Profile of the dimensionless displacement field for the second gradient model for  $f_1 = 2.236$  and different values of  $L_c = \{0.01, 0.1, 0.2, 0.4, 1000\}$ . Note that the deviation from the linear distribution due to the boundary conditions is maximal for  $L_c \rightarrow \infty$  (also equivalent to  $h \rightarrow 0$ )

while the equilibrium equations without body forces are the following:

$$\text{Div} \left[ 2\mu_{\text{micro}} \text{sym} \nabla \mathbf{u} - \lambda_{\text{micro}} \text{tr} (\nabla \mathbf{u}) \mathbb{1} + \mu L_c^2 \text{Div} \left[ \nabla^2 \mathbf{u} \right] \right] = \mathbf{0}. \tag{54}$$

Due to the shear problem symmetry the following structure of  $\mathbf{u} = (u_1(x_2), 0, 0)^T$  has been chosen. The boundary conditions for the simple shear are the following:

$$\begin{aligned} u_1(x_2 = 0) &= 0, & u_1(x_2 = h) &= \gamma h, \\ u_1'(x_2 = 0) &= 0, & u_1'(x_2 = h) &= 0. \end{aligned} \tag{55}$$

After substituting the expression of the displacement field in Eq. (54), the non-trivial equilibrium equation reduces to the following:

$$\mu_{\text{micro}} u_1''(x_2) - \mu L_c^2 u_1^{(4)}(x_2) = 0. \tag{56}$$

After applying the boundary conditions to the solution of Eq. (56), it results that  $u_1(x_2)$  is:

$$\begin{aligned} u_1(x_2) &= \frac{\frac{L_c}{f_1 h} \left( \sinh \left( \frac{f_1(h - 2x_2)}{2L_c} \right) - \sinh \left( \frac{f_1 h}{2L_c} \right) \right) + \frac{x_2}{h} \cosh \left( \frac{f_1 h}{2L_c} \right)}{\cosh \left( \frac{f_1 h}{2L_c} \right) - \frac{2L_c}{f_1 h} \sinh \left( \frac{f_1 h}{2L_c} \right)} \gamma h, \\ f_1 &:= \sqrt{\frac{\mu_{\text{micro}}}{\mu}}. \end{aligned} \tag{57}$$

A plot of the displacement profile while varying  $L_c$  is shown in Fig. 7. The following relation is a measure of the higher-order stiffness

$$\mu^* = \frac{1}{1 - \frac{2L_c}{f_1 h} \tanh \left( \frac{f_1 h}{2L_c} \right)} \mu_{\text{micro}}. \tag{58}$$

which is shown in the Sect. 8 in Fig. 5. Note that here, the size-independent macroscopic shear stiffness  $\mu^*$  for  $L_c \rightarrow 0$  ( $h \rightarrow \infty$ ) is given by  $\mu_{\text{micro}}$ .

### 11 Limit cases for the relaxed micromorphic continuum

In this section, we will discuss the limit cases for the relaxed micromorphic model and in particular how it behaves for  $0 \leftarrow L_c \rightarrow \infty$ , and how to retrieve from it the Cosserat model (Sect. 11.3) and the indeterminate couple stress model (Sect. 11.4) as special cases.

#### 11.1 Limit case for $\mu_e \rightarrow \infty$

This limit implies that  $\text{sym} \mathbf{P} = \text{sym} \nabla \mathbf{u}$  and the classic linear elastic solution at the micro-scale ( $\mu_{\text{macro}} = \mu_{\text{micro}} \mu_e / (\mu_{\text{micro}} + \mu_e) = \mu_{\text{micro}}$ ) is retrieved:

$$u_1 \Big|_{\mu_e \rightarrow \infty} = \gamma x_2, \quad \mu^* \Big|_{\mu_e \rightarrow \infty} = \mu_{\text{micro}} \tag{59}$$

#### 11.2 Limit case for $\mu_c$

##### 11.2.1 $\mu_c \rightarrow 0$

The classic linear elastic solution at the macro-scale is retrieved:

$$u_1 \Big|_{\mu_c \rightarrow 0} = \gamma x_2, \quad \mu^* \Big|_{\mu_c \rightarrow 0} = \frac{\mu_{\text{micro}} \mu_e}{\mu_{\text{micro}} + \mu_e} = \mu_{\text{macro}} \tag{60}$$

11.2.2  $\mu_c \rightarrow \infty$

This limit implies that skew  $\mathbf{P} = \text{skew } \nabla \mathbf{u}$ . The solution has identical structure to Eq. (18) in which  $f_1$  and  $f_2$  are replaced with their limits ( $\widehat{f}_1 = \sqrt{\mu_e/\mu}$  and  $\widehat{f}_2 = \mu_{\text{micro}}/(\widehat{f}_1(\mu_e + \mu_{\text{micro}}))$ ). The following solution is retrieved:

$$\begin{aligned}
 u_1 \Big|_{\mu_c \rightarrow \infty} &= \frac{\widehat{f}_2 L_c \sinh\left(\frac{\widehat{f}_1(h-2x_2)}{L_c}\right) + \frac{2x_2}{h} \cosh\left(\frac{\widehat{f}_1 h}{L_c}\right) - \frac{\widehat{f}_2 L_c}{h} \sinh\left(\frac{\widehat{f}_1 h}{L_c}\right)}{\cosh\left(\frac{\widehat{f}_1 h}{L_c}\right) - \frac{\widehat{f}_2 L_c}{h} \sinh\left(\frac{\widehat{f}_1 h}{L_c}\right)} \frac{\gamma h}{2}, \\
 P_{21} \Big|_{\mu_c \rightarrow \infty} &= -\frac{\sinh\left(\frac{\widehat{f}_1 x_2}{L_c}\right) \sinh\left(\frac{\widehat{f}_1(h-x_2)}{L_c}\right)}{\cosh\left(\frac{\widehat{f}_1 h}{L_c}\right) - \frac{\widehat{f}_2 L_c}{h} \sinh\left(\frac{\widehat{f}_1 h}{L_c}\right)} \frac{\mu_{\text{micro}}}{\mu_e + \mu_{\text{micro}}} \gamma, \\
 P_{12} \Big|_{\mu_c \rightarrow \infty} &= \frac{\cosh\left(\frac{\widehat{f}_1 h}{L_c}\right) \mu_e + \sinh\left(\frac{\widehat{f}_1 x_2}{L_c}\right) \sinh\left(\frac{\widehat{f}_1(h-x_2)}{L_c}\right) \mu_{\text{micro}}}{\cosh\left(\frac{\widehat{f}_1 h}{L_c}\right) - \frac{\widehat{f}_2 L_c}{h} \sinh\left(\frac{\widehat{f}_1 h}{L_c}\right)} \frac{1}{\mu_e + \mu_{\text{micro}}} \gamma.
 \end{aligned}
 \tag{61}$$

The following relation is a measure of the higher-order stiffness

$$\mu^* \Big|_{\mu_c \rightarrow \infty} = \frac{1}{1 - \frac{\widehat{f}_2 L_c}{h} \tanh\left(\frac{\widehat{f}_1 h}{L_c}\right)} \frac{\mu_e \mu_{\text{micro}}}{\mu_e + \mu_{\text{micro}}}.
 \tag{62}$$

11.3 Limit case for  $\mu_{\text{micro}} \rightarrow \infty$  (Cosserat, Sect. 6)

This limit implies that sym  $\mathbf{P} = 0$ , therefore  $\mathbf{P} = \mathbf{A} \in \mathfrak{so}(3)$ . The solution has a similar structure to Eq. (18) in which  $f_2$  is replaced with its limit ( $\widetilde{f}_2 = \mu_c/(f_1(\mu_e + \mu_c))$ ), while  $f_1$  does not change. It is important to highlight that for this limit the solution for a Cosserat continuum is retrieved:

$$\begin{aligned}
 u_1 \Big|_{\mu_{\text{micro}} \rightarrow \infty} &= \frac{\widetilde{f}_2 L_c \sinh\left(\frac{f_1(h-2x_2)}{L_c}\right) + \frac{2x_2}{h} \cosh\left(\frac{f_1 h}{L_c}\right) - \frac{\widetilde{f}_2 L_c}{h} \sinh\left(\frac{f_1 h}{L_c}\right)}{\cosh\left(\frac{f_1 h}{L_c}\right) - \frac{\widetilde{f}_2 L_c}{h} \sinh\left(\frac{f_1 h}{L_c}\right)} \frac{\gamma h}{2}, \\
 P_{21} \Big|_{\mu_{\text{micro}} \rightarrow \infty} &= -P_{12} \Big|_{\mu_{\text{micro}} \rightarrow \infty} = -\frac{\sinh\left(\frac{f_1 x_2}{L_c}\right) \sinh\left(\frac{f_1(h-x_2)}{L_c}\right)}{\cosh\left(\frac{f_1 h}{L_c}\right) - \frac{\widetilde{f}_2 L_c}{h} \sinh\left(\frac{f_1 h}{L_c}\right)} \gamma,
 \end{aligned}
 \tag{63}$$

The following relation is a measure of the higher-order stiffness

$$\mu^* \Big|_{\mu_{\text{micro}} \rightarrow \infty} = \frac{1}{1 - \frac{\widetilde{f}_2 L_c}{h} \tanh\left(\frac{f_1 h}{L_c}\right)} \mu_e.
 \tag{64}$$

11.4 Limit case for  $\mu_{\text{micro}} \rightarrow \infty$  and  $\mu_c \rightarrow \infty$  (indet. couple stress, Sect. 7)

These limits imply that sym  $\mathbf{P} = 0$  and that skew  $\mathbf{P} = \text{skew } \nabla \mathbf{u}$ . The solution has a similar structure to Eq. (18) in which  $f_1$  and  $f_2$  are replaced with their limits ( $\overline{f}_1 = 1/\overline{f}_2 = \sqrt{\mu_e/\mu}$ ). It is important to highlight that

for these limits, regardless the order in which they are taken, the solution for an indeterminate couple stress continuum is retrieved:

$$\begin{aligned}
 u_1 \Big|_{\mu_{\text{micro}} \rightarrow \infty} &= \frac{\frac{L_c}{\bar{f}_1 h} \sinh\left(\frac{\bar{f}_1(h-2x_2)}{L_c}\right) + \frac{2x_2}{h} \cosh\left(\frac{\bar{f}_1 h}{L_c}\right) - \frac{L_c}{\bar{f}_1 h} \sinh\left(\frac{\bar{f}_1 h}{L_c}\right)}{\cosh\left(\frac{\bar{f}_1 h}{L_c}\right) - \frac{L_c}{\bar{f}_1 h} \sinh\left(\frac{\bar{f}_1 h}{L_c}\right)} \frac{\gamma h}{2}, \\
 P_{21} \Big|_{\mu_{\text{micro}} \rightarrow \infty} &= -P_{12} \Big|_{\mu_{\text{micro}} \rightarrow \infty} = -\frac{\sinh\left(\frac{\bar{f}_1 x_2}{L_c}\right) \sinh\left(\frac{\bar{f}_1(h-x_2)}{L_c}\right)}{\cosh\left(\frac{\bar{f}_1 h}{L_c}\right) - \frac{L_c}{\bar{f}_1 h} \sinh\left(\frac{\bar{f}_1 h}{L_c}\right)} \gamma,
 \end{aligned} \tag{65}$$

The following relation is a measure of the higher-order stiffness:

$$\mu^* \Big|_{\mu_{\text{micro}} \rightarrow \infty} = \frac{1}{1 - \frac{L_c}{\bar{f}_1 h} \tanh\left(\frac{\bar{f}_1 h}{L_c}\right)} \mu_e. \tag{66}$$

## 11.5 Limit case for the characteristic length $L_c$

### 11.5.1 $L_c \rightarrow 0$

Similarly to the limit for  $\mu_c \rightarrow 0$ , the classic linear elastic solution at the macro-scale is retrieved:

$$\begin{aligned}
 u_1 \Big|_{L_c \rightarrow 0} &= \gamma x_2, \\
 \mu^* \Big|_{L_c \rightarrow 0} &= \frac{\mu_{\text{micro}} \mu_e}{\mu_{\text{micro}} + \mu_e} = \mu_{\text{macro}}.
 \end{aligned} \tag{67}$$

### 11.5.2 $L_c \rightarrow \infty$

This limit implies that  $\text{Curl} \mathbf{P} = 0$  which requires that  $\mathbf{P}$  has to be the gradient of a vector field  $\boldsymbol{\zeta}$  (see appendix of [36] for more details). Differently to the limit for  $\mu_e \rightarrow \infty$ , a classical linear elastic solution in between the micro- and the macro-scale is retrieved:

$$\begin{aligned}
 u_1 \Big|_{L_c \rightarrow \infty} &= \gamma x_2, \\
 \mu^* \Big|_{L_c \rightarrow \infty} &= \frac{(\mu_e + \mu_c) \mu_{\text{micro}}}{\mu_e + \mu_c + \mu_{\text{micro}}} < \mu_{\text{micro}}.
 \end{aligned} \tag{68}$$

## 12 Discussion

From the previous sections, it is possible to see how the shear stiffness behaves when the ratio between the thickness and the characteristic length  $h/L_c$  and the other elastic parameters tend to infinity or to zero. The Cosserat model, the classical micromorphic model (excluding when it collapse to the second gradient model), and the microstrain model cannot be distinguished qualitatively from the size effect under simple shear, but they exhibit a qualitatively different behavior for thin specimens under bending [13,35,37]. Contrary to all the other models seen in this work, the relaxed micromorphic model is always bounded, with the only exception for the limit of  $\mu_{\text{micro}} \rightarrow \infty$  when  $h/L_c \rightarrow 0$ , since the relaxed micromorphic model then degenerates into the Cosserat model which in turn collapses itself into the indeterminate couple stress model. The relaxed micromorphic model shows also a good balance between the complexity of its solution and the amount of work required in order to obtain that simple and manageable explicit solution (contrary to the classical micromorphic



model and the micro-strain model), the physical reasonableness of having a bounded shear stiffness regardless the value of the ratio  $h/L_c$  (contrary to the Cosserat model, the indeterminate couple stress model and, the second gradient model), and the freedom given by having more than one elastic parameter (contrary to the indeterminate couple stress model and the second gradient model).

### 13 Summary and conclusions

In the present paper, closed-form solutions of the simple shear problem have been derived for several isotropic linear-elastic micromorphic models, namely for the relaxed micromorphic continuum, the Cosserat continuum, a fully micromorphic continuum and a micro-strain continuum.

Limiting cases like the strain-gradient continuum and the indeterminate couple-stress continuum are considered. Both of the latter show an unbounded shear stiffness if the height of the shear strip becomes very small compared to the intrinsic length  $L_c$ , which is a physically questionable prediction. In contrast, the stiffness remains bounded for the unconstrained micromorphic models.

Furthermore, the derived solutions show the individual effect of each of the constitutive parameters on the effective shear stiffness of a thin layer. Consequently, these solutions offer a way to calibrate the constitutive parameters, except the bulk moduli, from a series of respective real or virtual shear experiments with a number of specimens of different height  $h$ . In this context, it shall be pointed out that the unconstrained models (relaxed micromorphic, Cosserat, micro-strain and full micromorphic) yield qualitatively comparable results, so that a parameter set can be presumably calibrated for each of these models from a series of the aforementioned shear experiments. However, the predictions of these models will differ for size effects under other loading conditions. It is thus an important future task to find and compare the predictions of these models for other loading conditions, like bending or torsion, and to compare their predictions with respective (real or virtual) experiments and to derive guidelines for a favorable choice among the numerous available micromorphic continuum models.

**Acknowledgements** AM acknowledge funding from the French Research Agency ANR, “METASMART” (ANR-17CE08-0006). AM and GR acknowledges support from IDEXLYON in the framework of the “Programme Investissement d’Avenir” ANR-16-IDEX-0005.

### Compliance with ethical standards

**Conflict of interest** The authors declared that they have no conflicts of interest to this work.

### References

1. Aifantis, E.C.: The physics of plastic deformation. *Int. J. Plast* **3**(3), 211–247 (1987)
2. Aifantis, K.E., Willis, J.R.: The role of interfaces in enhancing the yield strength of composites and polycrystals. *J. Mech. Phys. Solids* **53**(5), 1047–1070 (2005)
3. Cosserat, E., Cosserat, F.: *Théorie des Corps déformables*. Hermann, Paris (1909)
4. d’Agostino, M.V., Barbagallo, G., Ghiba, I.D., Eidel, B., Neff, P., Madeo, A.: Effective description of anisotropic wave dispersion in mechanical band-gap metamaterials via the relaxed micromorphic model. *J. Elas* **139**, 299 (2019)
5. Diebels, S., Steeb, H.: Stress and couple stress in foams. *Comput. Mater. Sci.* **28**(3–4), 714–722 (2003)
6. Dunn, M., Wheel, M.: Size effect anomalies in the behaviour of loaded 3d mechanical metamaterials. *Phil. Mag.* **100**(2), 139–156 (2020)
7. Eringen, A. C.: Mechanics of micromorphic continua. In: *Mechanics of Generalized Continua*, pp. 18–35. Springer, Berlin (1968)
8. Forest, S.: Generalized continua from the theory to engineering applications. In: Altenbach, H., Eremeyev, V. (eds.) *Micromorphic Media*, vol. 541, pp. 249–300. Springer, Berlin (2013)
9. Forest, S.: Questioning size effects as predicted by strain gradient plasticity. *J. Mech. Behavior Mater.* **22**(3–4), 101–110 (2013)
10. Forest, S.: Micromorphic approach to materials with internal length. In: *Encyclopedia of Continuum Mechanics*, pp. 1–11. Springer, Berlin, Heidelberg (2018)
11. Forest, S., Sievert, R.: Nonlinear microstrain theories. *Int. J. Solids Struct.* **43**(24), 7224–7245 (2006)
12. Hadjesfandiari, A.R., Dargush, G.F.: Couple stress theory for solids. *Int. J. Solids Struct.* **48**(18), 2496–2510 (2011)
13. Hütter, G.: Application of a microstrain continuum to size effects in bending and torsion of foams. *Int. J. Eng. Sci.* **101**, 81–91 (2016)
14. Hütter, G.: On the micro-macro relation for the microdeformation in the homogenization towards micromorphic and micropolar continua. *J. Mech. Phys. Solids* **127**, 62–79 (2019)

15. Hütter, G., Mühlich, U., Kuna, M.: Micromorphic homogenization of a porous medium: elastic behavior and quasi-brittle damage. *Continuum Mech. Thermodyn.* **27**(6), 1059–1072 (2015)
16. Ilchev, A., Marcadon, V., Kruch, S., Forest, S.: Computational homogenisation of periodic cellular materials: application to structural modelling. *Int. J. Mech. Sci.* **93**, 240–255 (2015)
17. Jeong, J., Neff, P.: Existence, uniqueness and stability in linear Cosserat elasticity for weakest curvature conditions. *Math. Mech. Solids* **15**(1), 78–95 (2010)
18. Kruch, S., Forest, S.: Computation of coarse grain structures using a homogeneous equivalent medium. *Le Journal de Physique IV* **8**(PR8), Pr8–197 (1998)
19. Liebenstein, S., Sandfeld, S., Zaiser, M.: Size and disorder effects in elasticity of cellular structures: from discrete models to continuum representations. *Int. J. Solids Struct.* **146**, 97–116 (2018)
20. Madeo, A., Ghiba, I.D., Neff, P., Münch, I.: A new view on boundary conditions in the Grioli-Koiter-Mindlin-Toupin indeterminate couple stress model. *Euro. J. Mech.-A/Solids* **59**, 294–322 (2016)
21. Mazière, M., Forest, S.: Strain gradient plasticity modeling and finite element simulation of Lüders band formation and propagation. *Continuum Mech. Thermodyn.* **27**(1–2), 83–104 (2015)
22. Mindlin, R.D.: Micro-structure in linear elasticity. *Arch. Ration. Mech. Anal.* **16**(1), 51–78 (1964)
23. Münch, I., Neff, P., Madeo, A., Ghiba, I.D.: The modified indeterminate couple stress model: why Yang et al.’s arguments motivating a symmetric couple stress tensor contain a gap and why the couple stress tensor may be chosen symmetric nevertheless. *Z. Angew. Math. Me.* **97**(12), 1524–1554 (2017)
24. Neff, P.: On material constants for micromorphic continua. In: *Trends in Applications of Mathematics to Mechanics, STAMM Proceedings*, Seeheim, pp. 337–348. Shaker-Verlag (2004)
25. Neff, P.: The Cosserat couple modulus for continuous solids is zero viz the linearized Cauchy-stress tensor is symmetric. *Z. Angew. Math. Me.* **86**(11), 892–912 (2006)
26. Neff, P., Eidel, B., d’Agostino, M.V., Madeo, A.: Identification of scale-independent material parameters in the relaxed micromorphic model through model-adapted first order homogenization. *J. Elast.* **139**, 269–298 (2020)
27. Neff, P., Ghiba, I.D., Madeo, A., Placidi, L., Rosi, G.: A unifying perspective: the relaxed linear micromorphic continuum. *Continuum Mech. Thermodyn.* **26**(5), 639–681 (2014)
28. Neff, P., Jeong, J.: A new paradigm: the linear isotropic Cosserat model with conformally invariant curvature energy. *Z. Angew. Math. Me.* **89**(2), 107–122 (2009)
29. Neff, P., Jeong, J., Fischle, A.: Stable identification of linear isotropic Cosserat parameters: bounded stiffness in bending and torsion implies conformal invariance of curvature. *Acta Mech.* **211**(3–4), 237–249 (2010)
30. Neff, P., Münch, I.: Simple shear in nonlinear Cosserat elasticity: bifurcation and induced microstructure. *Continuum Mech. Thermodyn.* **21**(3), 195–221 (2009)
31. Neff, P., Münch, I., Ghiba, I.D., Madeo, A.: On some fundamental misunderstandings in the indeterminate couple stress model. A comment on recent papers of AR Hadjesfandiari and GF Dargush. *Int. J. Solids Struct.* **81**, 233–243 (2016)
32. Nourmohammadi, N., O’Dowd, N.P., Weaver, P.M.: Effective bending modulus of thin ply fibre composites with uniform fibre spacing. *Int. J. Solids Struct.* **196**, 26 (2020)
33. Pham, R.D., Hütter, G.: Influence of topology and porosity on size effects in cellular materials with hexagonal structure under shear, tension and bending. *arXiv preprint arXiv:2009.10404* (2020)
34. Rizzi, G., Dal Corso, F., Veber, D., Bigoni, D.: Identification of second-gradient elastic materials from planar hexagonal lattices. part ii: Mechanical characteristics and model validation. *Int. J. Solids Struct.* **176**, 19–35 (2019)
35. Rizzi, G., Hütter, G., Madeo, A., Neff, P.: Analytical solutions of the cylindrical bending problem for the relaxed micromorphic continuum and other generalized continua (including full derivations). *arXiv preprint* (2020)
36. Rizzi, G., Hütter, G., Madeo, A., Neff, P.: Analytical solutions of the simple shear problem for certain types of micromorphic continuum models—including full derivations. *arXiv preprint arXiv:2006.02391* (2020)
37. Rueger, Z., Lakes, R.S.: Experimental study of elastic constants of a dense foam with weak Cosserat coupling. *J. Elast.* **137**(1), 101–115 (2019)
38. Shaat, M.: A reduced micromorphic model for multiscale materials and its applications in wave propagation. *Compos. Struct.* **201**, 446–454 (2018)
39. Tekoğlu, C., Onck, P.R.: Size effects in two-dimensional voronoi foams: a comparison between generalized continua and discrete models. *J. Mech. Phys. Solids* **56**(12), 3541–3564 (2008)
40. Yoder, M., Thompson, L., Summers, J.: Size effects in lattice-structured cellular materials: material distribution. *J. Mater. Sci.* **54**(18), 11858–11877 (2019)
41. Zhang, Z., Liu, Z., Gao, Y., Nie, J., Zhuang, Z.: Analytical and numerical investigations of two special classes of generalized continuum media. *Acta Mech. Solida Sin.* **24**(4), 326–339 (2011)